FIZIKA 21$_{st}$ (1989), Supplement 2, 1-16
(Proc. Gst Adriatic Meeting on Particle Physics,
Modern Trends in Particle Physics '89, Dubrovnik,
Dubrovnik, June 1989)

STATUS OF t-QUARK SEARCHES AT HADRON COLLIDERS AND PRESENT MASS LIMITS

Presented by D. Denegri (UA1 Collaboration)

CERN, Geneva, Switzerland
and
DPhPE CEN-Saclay, Gif-sur-Yvette, France

(I dedicate this lecture to the memory of my mother.)

ABSTRACT

We discuss the present top-quark searches and the lower limits on the top mass from the CERN and Fermilab collider experiments, and what may be expected from the latest data-taking periods of 1988/89. With the data of 1989, the mass domain probed extends up to $m_t \sim m_W$; we discuss some aspects of this t-quark mass range, some experimental hints, and the physics background of W + $\geq$ 2-jet events.

1. INTRODUCTION

Figure 1 shows the t-quark production regime of the UA1 and UA2 experiments at $\sqrt{s}$ = 0.63 TeV, expressed in terms of the number of top events with a semileptonic decay (BR = 1/9), for two values of the experimental sensitivity. Three domains can be distinguished: for $m_t \lesssim 45$ GeV the main mechanism is $t\bar{t}$ production; for $45 \lesssim m_t \lesssim m_W$ the dominant contribution is from $W \rightarrow t\bar{b}$, and for $m_t > m_W$ only $t\bar{t}$ contributes, with in this case a two-body t-quark decay $t \rightarrow W\bar{b}$ with an on-shell W.

Figure 1 also shows the present lower limits on m_t: the older PETRA limit at 23 GeV, and the most recent TRISTAN limit at 29.2 GeV [1, 2]. The limit is based on the non-observation of the expected rise in the ratio $R = \sigma_{had}/\sigma^{\gamma}_{\mu\mu}$ had the open t-production threshold been crossed, and the absence of excess 'spherical' events. Also shown is the published UA1 limit: $m_t > 41$ GeV [3, 4] obtained from the analysis of the e/μ + jets data collected by UA1 between 1983 and 1985.

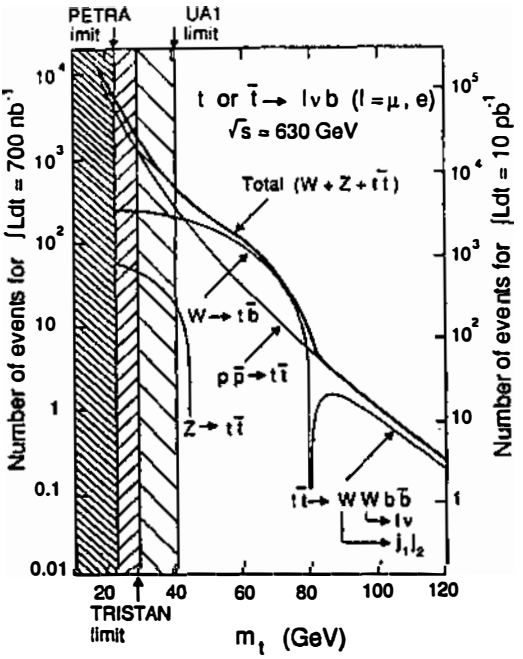

Fig. 1 Number of semileptonic decay top events, as a function of m_t at $\sqrt{s}$ = 0.63 TeV, for an integrated luminosity of 0.7 events per picobarn (data of up to and including 1985), left-hand scale, and for 10 events per picobarn, right-hand scale. No experimental cuts or efficiencies are included.

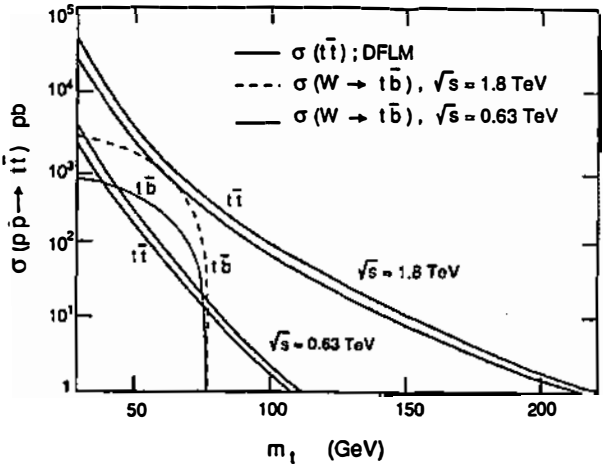

Fig. 2 The $p\bar{p} \to t\bar{t}$ and $p\bar{p} \to W \to t\bar{b}$ cross-sections at $\sqrt{s}$ = 0.63 and 1.8 TeV. The $t\bar{t}$ production is according to Refs. [4] and [5] with DFLM structure functions.

The t-quark mass ranges that can be explored, with data recorded in 1988 by experiments UA1, UA2, and CDF, extend into the 50 to 60 GeV range, and with the data of 1989 into the ~ 70 GeV range for UA1 and UA2 and ~ 80 to ~ 90 GeV for CDF.

Figure 2 compares the $t\bar{t}$ and $t\bar{b}$ cross-sections at $\sqrt{s}$ = 0.63 and 1.8 TeV [4, 5]. At 1.8 TeV, $t\bar{t}$ is dominant for any value of m_t, and Fermilab has a substantial advantage in cross-section for $m_t > m_W$—a factor of > 25; for $m_t \lesssim m_W$, however, as the $W \rightarrow t\bar{b}$ contribution is predominant at $\sqrt{s}$ = 0.63 TeV (Figs. 1 and 2), the advantage of the Fermilab collider is a factor of ~ 4 to ~ 10, depending on m_t.

2. SIGNATURES AND EVENT TOPOLOGIES USED BY UA1, UA2, AND CDF

All three experiments rely on the semileptonic $t \rightarrow e/\mu + \nu + b$ decay-mode signature, with an isolated e or μ, well separated from the remaining b-fragments owing to the large Q-value in the t-quark decay. The e and/or μ is used for trigger and event selection, the neutrino (E_T^{miss}) for background suppression (by UA2 and CDF), and there is a topological cut of at least two accompanying jets in order to make a further reduction in the background in the single charged-lepton channels. The UA1 experiment in the 1988/89 data-taking periods has only a μ detection capability, the UA2 can detect only electrons, whereas CDF has both e and μ detection.

The final states investigated until now are the following:

In UA1, the two channels used are: $\mu_{isol} + \geq 2$ jets and $\mu_{isol} + \mu_{in\ jet} + \geq 1$ jet [6]. The equal-sign dimuon channel, fed by (first generation) $W \rightarrow t\bar{b}$ decays, provides an appropriate signature for the t-quark mass range now being investigated, i.e. $40 \lesssim m_t \lesssim 70$ GeV, where $W \rightarrow t\bar{b}$ dominates (Fig. 1). This channel may seem more limited by statistics owing to the two semileptonic decays required. However, this is partly compensated by the lower instrumental and physics backgrounds for dimuons, allowing lower p_T^{μ} trigger and selection cuts (Table 1).

In UA2, two analyses are performed: one selecting $e + \nu + \geq 2$ jets (the electron is always isolated for instrumental reasons), the other with $e_{tight} + \nu + \geq 2$ jets, where tighter requirements are imposed on the instrumental electron signature (for example, the response of the transition radiation detector) [7]. To compensate for the decrease in $e^{\pm}$ detection efficiency, the E_T^{miss} cut is relaxed in the latter case. The UA2 experiment has also the possibility of exploiting the $e + e + \nu$ + jets final state. As, in practice, the electron transverse energy trigger/detection/selection threshold cuts are usually higher than for dimuons, the sensitivity of the dielectron channel is limited to a lower mass region, $m_t \lesssim 40$ GeV.

In CDF, two final states have been exploited so far: $e + \mu + X$ and $e + \nu + \geq 2$ jets [8, 9]. The $e\mu$ channel, where both the e and μ are isolated since they come from massive t-quark $t\bar{t}$ production, has the great advantage of providing a clean signature with little experimental background. The background comes from $Z \rightarrow \tau\bar{\tau}$ and residual $b\bar{b}$ production, the latter being heavily suppressed by lepton isolation and $p_T^{e,\mu}$ threshold cuts. In spite of the unfavourable branching ratios, and of a large additional suppression factor (of the order of ~ 20) due to lepton p_T and geometrical acceptance cuts ($|\eta_{lepton}| < 1$) and to the lepton detection/recognition efficiencies (Fig. 3), the $e\mu$ channel is still competitive owing to the much larger $t\bar{t}$ cross-section at $\sqrt{s}$ = 1.8 TeV (Fig. 2). The $e + \nu + \geq 2$-jet final state, also studied by CDF, is less limited by statistics and may already allow the $m_t \sim m_W$ region to be probed, but it suffers from larger backgrounds. The CDF experiment has, in addition, the possibility of studying the $\mu + \nu + \geq 2$ jets, $\mu + \mu$ + jets, and $e + e$ + jets channels [9].

Table 1

Selection cuts in the main channels of UA1, UA2, and CDF used in the search for the t-quark; the dominant backgrounds are indicated.

UA1	UA2	CDF
μ_{isol} + ≥ 2 jets:	e_{isol} + ν + ≥ 2 jets:	e_{isol} + μ_{isol} + X:
$p_T^{\mu} > 12$ GeV/c	$E_T^e \geq 11.5$ GeV	$E_T^e \geq 15$ GeV
$\lvert\eta_\mu\rvert < 1.7$	$\lvert\eta_e\rvert < 1.0$	$\lvert\eta_e\rvert < 1.0$
$E_T^{jet_1} > 15$ GeV	$E_T^{miss} > 15$ GeV	$p_T^{\mu} > 12$ GeV/c
$E_T^{jet_2} > 7$ GeV	$E_T^{jet_1} > 10$ GeV	$\lvert\eta_\mu\rvert < 1.2$
$m_T^{\mu\nu} < 60$ GeV	$E_T^{jet_2} > 8$ GeV	e_{isol} + ν + ≥ 2 jets:
μ_{isol} + $\mu_{in\ jet}$ + jets:	e_{isol}^{tight} + ν + ≥ 2 jets:	$E_T^e > 20$ GeV
$\mu_{isol} > 8$ GeV/c	Same, except:	$E_T^{miss} > 20$ GeV
$\mu_{in\ jet} > 3$ GeV/c	$E_T^{miss} > 10$ GeV	$E_T^{jets} > 10$ to 20 GeV
$E_T^{jet} > 10$ GeV		
Backgrounds:		
$b\bar{b}g$, $\pi/K \rightarrow \mu$,	W + 2 jets	$e\mu$: $b\bar{b}$, $\tau\bar{\tau}$
W + 2 jets		$e\nu$ jets: W + 2 jets

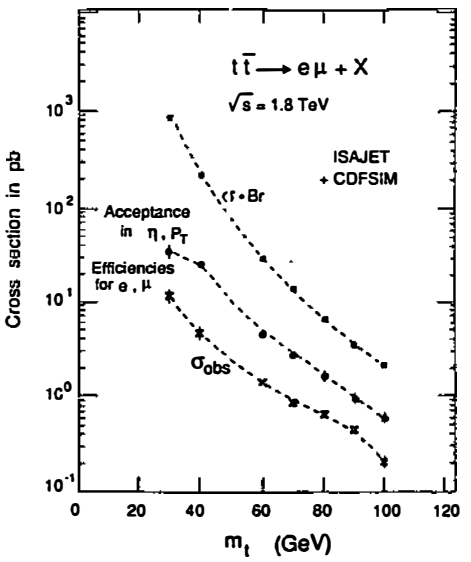

Fig. 3 Reduction of the $t\bar{t} \rightarrow e\mu + X$ cross-section due to acceptance and efficiency cuts in the experimental conditions of CDF [9].

3. SELECTION CUTS USED BY UA1, UA2, AND CDF

The integrated luminosities recorded are: ~ 1.3 pb^{-1} in 1988 and ~ 3.4 pb^{-1} in 1989 for UA1; ~ 2.5 pb^{-1} in 1988 and ~ 4.0 pb^{-1} in 1989 for UA2; and ~ 4.7 pb^{-1} for the year-long CDF run of 1988/89. So far, only the data from 1988 have been (partly) analysed.

The specific cuts applied by the three experiments are summarized in Table 1. We also indicate the expected dominant backgrounds for the chosen cuts. Notice that, contrary to UA2 and CDF, UA1 has no E_T^{miss} cut in the lepton + ≥ 2-jet channel. This is due to the poorer E_T^{miss} resolution when a muon, rather than an electron, is used. Thus the dominant physics background for UA1 is $b\bar{b}g$ production. For UA2 and CDF, the cuts on $E_T^{miss} > 15$ and 20 GeV, respectively, make the $b\bar{b}$ background negligible, and the only physics background to consider is $W(\rightarrow e + \nu) + \geq 2$-jet production). This background can in turn be suppressed with cuts on the $e\nu$ (or $\mu\nu$) transverse mass: typically $m_T^{e\nu} < 50$ or 60 GeV [7, 9]. However, this cut may limit the sensitivity at the upper end of the m_t range searched for, and must be removed if $m_t \sim m_W$, where a different method must be used. An important source of instrumental background for UA1 is also due to $\pi/K \rightarrow \mu$ decays. Notice (Table 1) the low p_T^{μ} cuts used by UA1 in the dimuon channel; these are necessary in order to pick up the softer b-decay muons from $W \rightarrow t\bar{b}$, and to still remain competitive despite the two semileptonic decays. For the $e\mu$ channel of CDF, the only significant background is $b\bar{b}$ followed by two semileptonic decays. It can be seen that the jet cuts are similar in all three experiments, $E_T^{jet} \geq$ 10 GeV, with $|\eta_{jet}| < 2.0$ to 2.5.

4. METHODS EMPLOYED AND RESULTING MASS LIMITS

4.1 The analysis of UA1

In the $\mu + \geq 2$-jet channel the method consists in measuring the absolute rate of isolated muon events. This is possible only with muons, for which the isolation distribution can be studied; more specifically, the transition from non-isolated muons to the regime where they are highly isolated, and where a t-quark contribution is possible. UA1 has a good understanding of its muon production [3, 6, 10], and of the muon isolation in particular (Fig. 4). The isolation variable I is defined as $I = [(\Sigma E_T/3)^2 + (\Sigma p_T/2)^2]^{1/2}$, where ΣE_T and Σp_T are the energy and momentum flows measured around the muon track, in a cone of half-opening angle $\Delta R = [\Delta\eta^2 + \Delta\phi^2]^{1/2} = 0.7$. The data in Fig. 4 are compared with the expected distribution for the various physics ($b\bar{b}g$, W + ≥ 2 jets, etc.) and instrumental ($\pi/K \rightarrow \mu$ decays) backgrounds, and with the expected contribution for a 40 GeV t-quark. From the absence of excess isolated muons in the $I \leq 2$ bin, and with the background shape normalized to data at $I \geq 2$, UA1 obtains a lower limit $m_t \geq 44$ GeV (95% CL).

The dimuon + jet events yield an independent limit of $m_t \geq 43$ GeV (95% CL). This limit is obtained from the dimuon event rate and the shape of kinematical distributions. A likelihood variable L is defined, incorporating the expected signal and background shapes; no events are observed in a region where the t-quark contribution is expected to dominate, and where, for example, 3.2 events are expected for $m_t = 40$ GeV [6].

UA1 thus finds no evidence for t-quark production in either channel. Combining all available data (up to and including 1988 data) on e + jets, μ + jets, $\mu\mu$ + jets, and e + μ, and from the comparison between the upper bound on the possible t-quark contribution and the expected t-quark production cross-section [4, 5] (Fig. 5), lower limits on the t-quark mass are obtained: $m_t > 56$ GeV at 95% CL and $m_t > 60$ GeV at 90% CL [6].

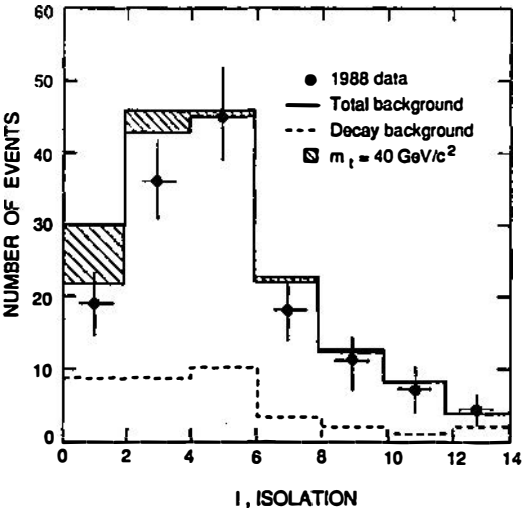

Fig. 4 The muon isolation I distribution in μ + ≥ 2-jet events of UA1; data of 1988 [6].

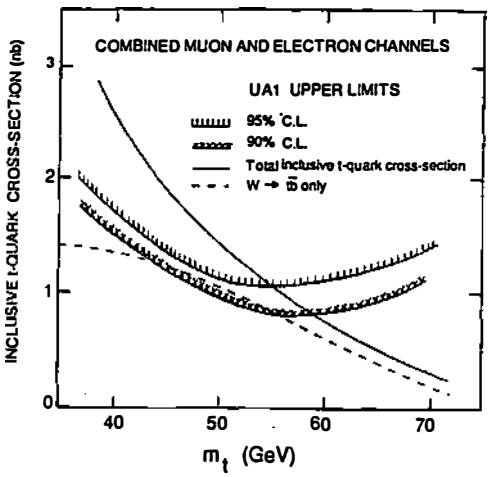

Fig. 5 Upper limit on the t-quark production cross-section from UA1 data [6], compared with the expected t-quark production [4, 5].

4.2 The analysis of UA2

The analysis of UA2 in the e + ν + ≥ 2-jet channel relies on the shape of the eν transverse mass distribution $m_T^{e\nu} = [2E_T^e E_T^\nu (1 - \cos \Delta\phi_{e\nu})]^{1/2}$, and on the observed event rate in the $m_T^{e\nu}$ region where the t-quark signal to W + ≥ 2-jet background ratio is optimal. Figure 6 shows the expected shape of the $m_T^{e\nu}$ distribution for a 60 GeV t-quark: a) for $t\bar{t}$ production, b) for $t\bar{b}$ production, and c) for the background of W + 2-jet events, obtained with the Ellis-Kleiss-Stirling (EKS) Monte Carlo

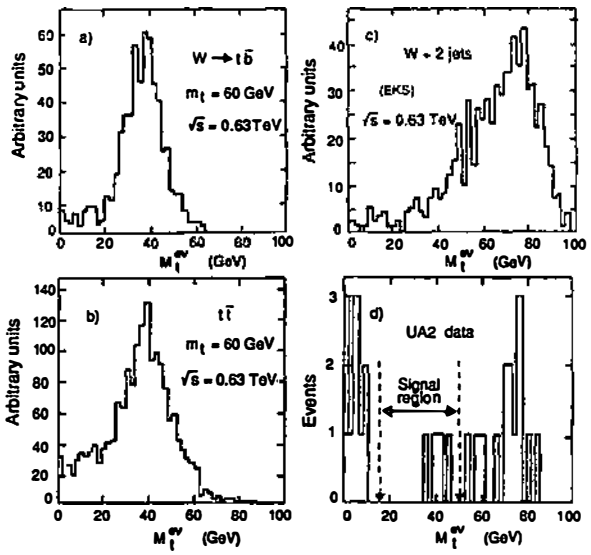

Fig. 6 The $e\nu$ transverse mass distributions: a) and b) for t-quark production with $m_t = 60$ GeV, c) for $W(\rightarrow e\nu) + 2$ jets, and d) for the $e + \nu + \geq 2$-jet data of UA2. The histograms in (a), (b), and (c) are after full simulation of the UA2 detector response [7].

[11]. The region chosen for the t-quark search is $15 \leq m_T^{e\nu} \leq 50$ GeV. The data of UA2 are shown in Fig. 6d [7], and are consistent with W + 2 jets, i.e. there is no evidence for t-quark production. Normalizing the background shape to the data at $m_T^{e\nu} > 50$ GeV, and from the statistical analysis of the observed and expected number of events in the $15 \leq m_T^{e\nu} \leq 50$ GeV region—taking into account statistical and systematic uncertainties from the energy scale of electrons, neutrinos, and jets, and in the background—UA2 comes to the conclusion that there is no indication for a t-quark in the region $40 < m_t < 60$ GeV [7].

4.3 The analysis of CDF

The present analysis corresponds to an experimental sensitivity of ~ 2.5 events per picobarn, and is still at a preliminary stage [9]. In the $e\mu$ channel the method is based on the observed event rate. Figures 7a–c show the scatter-plot of the electron versus muon transverse momenta, with the required isolation criteria, for a 40 and 60 GeV t-quark in (a) and (b) respectively, and for the $b\bar{b}$ background in (c). The data are shown in Fig. 7d. The selected signal region is $E_T^e \geq 15$ GeV and $p_T^\mu > 12$ GeV/c. From the observation of zero $e\mu$ events in this region and with the expected $t\bar{t}$ (+ $t\bar{b}$) event rate, taking into account statistical and systematic uncertainties, the CDF Collaboration concludes that the t-quark is unlikely in the $30 < m_t < 60$ GeV mass range [9].

In the $e + \nu + \geq 2$-jet channel, the CDF analysis is based on the shape of the $e\nu$ transverse mass $m_T^{e\nu}$ and observed event rates, and is very similar to the analysis of UA2. The cuts $E_T^{e\nu} \geq 20$ GeV (Table 1) are somewhat harder than in UA2, and the only significant background is W + 2 jets. In Figs. 8a,b we show the expected shape of $m_T^{e\nu}$: a) for a 70 GeV t-quark, b) for W + 2 jets; Fig. 8c shows the data. The optimal signal region is now $10 \leq m_T^{e\nu} \leq 60$ GeV. Again there is no evidence for t-quark production. From the comparison between the data and the expected signal and background

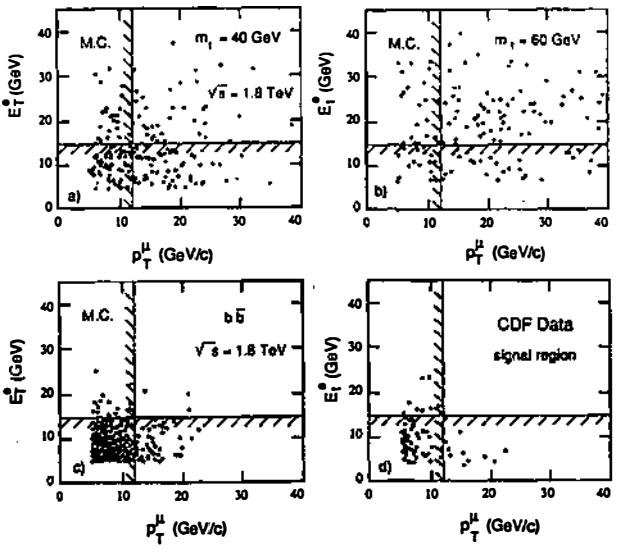

Fig. 7 Isolated electron versus muon transverse momenta at 1.8 TeV: a) and b) for m_t = 40 and 60 GeV, respectively; c) for the $b\bar{b}$ background; d) for the CDF data in the $e\mu$ channel. Monte Carlo distributions in (a), (b), and (c) are with full detector simulation, and correspond to integrated luminosities of 10, 50, and 10 pb^{-1}, respectively. The data are for 2.3 pb^{-1} [9].

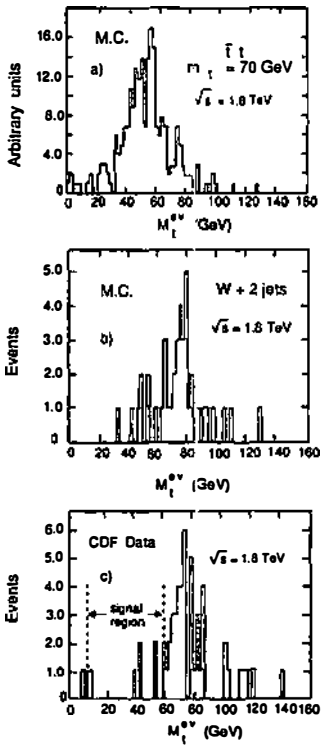

Fig. 8 The $e\nu$ transverse mass distributions at 1.8 TeV: a) from t-quark production; b) from $W(\rightarrow e\nu)$ + 2 jets; c) for the e + ν + $\geq$ 2-jet data of CDF. The histograms in (a) and (b) are after full simulation of the CDF detector response [9].

shapes, the conclusion from a preliminary analysis (the effects of systematics on low-E_T jets not yet accounted for) is that a t-quark in the $45 < m_t < 60$ GeV range is unlikely [9].

The three experiments thus come to the same conclusion: that the t-quark is most likely above ~ 60 GeV (the analyses are not yet final, however). The results are based on 1988 data. With the data of 1989 the experiments are approaching and probing the region $m_t \sim m_W$, which is interesting since there are some experimental hints [12–14], and as a number of theoretical models and phenomenological analyses favour a t-quark in this mass range [15].

5. TOP PRODUCTION AND DECAY FOR $m_t \sim m_W$

5.1 Cross-sections and event signatures

As the mass of the t-quark increases, we approach the regime where it decays into an on-shell W and a b-quark ($t \to Wb$) [12, 14, 16, 17]. The transverse mass of the lepton–neutrino system varies rapidly with m_t, until for $m_t \gtrsim 90$ GeV it becomes indistinguishable from direct W decays. For $m_t \gtrsim 75$ GeV, $t\bar{t}$ production is the only significant production mechanism left, giving thus $WWb\bar{b}$ final states. In the $m_t \approx m_W$ threshold region, this final state is characterized by a large transverse momentum $p_T^t \sim p_T^W \sim m_t/2$ and highly unbalanced transverse momenta $p_T^W \gg p_T^b$. For $75 \lesssim m_t \lesssim 110$ GeV, the soft ($E_T \sim 10$ GeV) b-quark jets are difficult to observe. The t-quark events must then be searched for in a $W(\to \ell\nu)$ production sample, with a W accompanied by at least two hard (W decay) jets.

With an experimental sensitivity of ~ 30 events per picobarn, the mass reach of the CERN Collider extends up to ~ 100 GeV. It is clear from Fig. 2—and from Fig. 9, which shows the energy dependence of $t\bar{t}$ production [22] from CERN to Fermilab energies—that Fermilab has a substantial

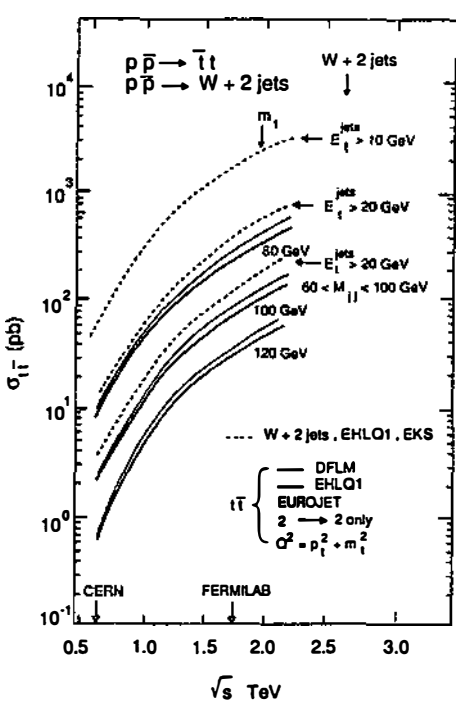

Fig. 9 The $t\bar{t}$ signal and W + 2-jet background cross-sections as a function of $\sqrt{s}$, for $80 < m_t < 120$ GeV. The $t\bar{t}$ cross-section is calculated with the EUROJET [18] Monte Carlo; the W + 2-jet cross-section with the EKS Monte Carlo [11]. Three sets of cuts on jets are indicated, and $|\eta_{jet}| < 2.5$.

advantage, its mass reach extending up to ~ 150 GeV for a comparable luminosity. The question is, however, whether the t-quark signal in the $\ell + \nu + \geq 2$-jet channel can be separated from the single-W + ≥ 2-jet background, also shown in Fig. 9. The $e\mu$ channel is not plagued by this background, but is more limited in mass, allowing to go up to ~ 100 GeV.

5.2 Hints from the data and the W + 2-jet background

In the data of 1985, UA2 observed one and UA1 two large-p_T $W(\rightarrow \ell\nu)$ events accompanied by two hard jets with $M_{jet\text{-}jet} \approx m_W$ [13, 19]. These events were suggestive of $t\bar{t}$ production, and with experimental sensitivities of ~ 1 event per picobarn and detection efficiencies of $\epsilon_W \sim 0.5$, the expected number of events varied from ~ 1.8 to ~ 0.4 (per W leptonic mode), with m_t increasing from 75 to 95 GeV. The observed event rate would favour the lower part of this mass range. UA1's problem concerning the $t\bar{t}$ interpretation was the value of p_T^W (≥ 65 GeV), which was too high [13]. However, taking into account the resolution and the systematic uncertainty on p_T^W, the $t\bar{t}$ interpretation was still marginally tenable [14].

The alternative interpretation was single-W + 2-jet production. For UA2, the rate and kinematical configuration of their only WW-consistent event was compatible with single-W production [20], whilst for UA1 the problem was again that the values of p_T^W were too large [13]. The situation is summarized in Fig. 10, showing the jet-jet effective mass versus p_T^W for all W + ≥ 2-jet events of UA1 [13]. The event population, compared with the expected W + 2-jet production, is properly clustered in the expected most probable region of the plot, with the two WW-consistent events labelled A and B. The expected number of events in this kinematical region is ~ 0.05 [13], and for t-quark production it is ~ 0.07 to 0.02, depending on m_t, with a factor of ~ 1.4 uncertainty. The contours in Fig. 10 are for the UA1 jet acceptance, since it differs significantly from that of UA2 before upgrading, the UA2 event (labelled C in the following) cannot be plotted in Fig. 10.

The W-jet-jet effective mass versus p_T^W plot for these three events, assuming a $t\bar{t}$ hypothesis, is shown in Fig. 11. The contours are again for UA1 acceptances, but event C is now included, as the

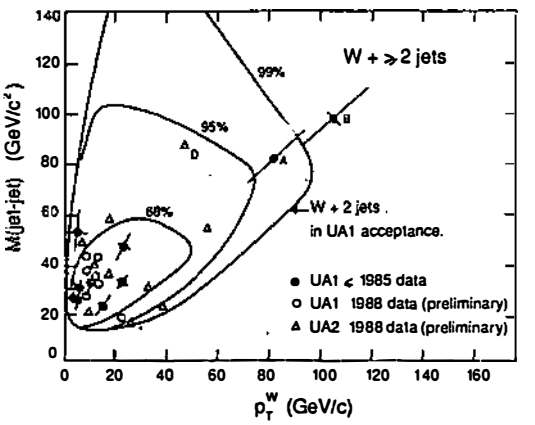

Fig. 10 Jet-jet effective mass versus p_T^W for all W + ≥ 2-jet events, compared with the expected QCD distribution, for data (up to and including 1988) of UA1 [6, 13, 14] and UA2 [20, 21]. The data of 1988 are still preliminary.

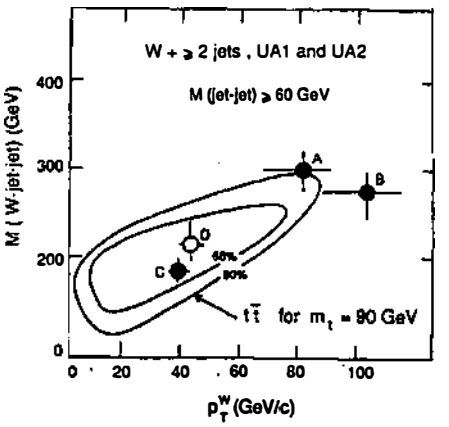

Fig. 11 WW effective mass versus p_T^W for $t\bar{t} \rightarrow WWb\bar{b}$ production, and events A, B, C, and D of UA1/2 (data up to and including 1988) consistent with apparent WW production [14].

effect of the difference between UA1 and UA2 acceptances must be small for the hard and central jets from a massive t-quark (W) decay. The sampling of the expected $t\bar{t}$ population provided by the three events together is not so bad.

5.3 UA1 and UA2 data of 1988

What is happening in the new data of 1988? The UA1 experiment obtained seven additional $W(\rightarrow \mu\nu) + \geq$ 2-jet events, with $E_T^{jet} \geq 7$ GeV and $|\eta_{jet}| < 2.5$ [6], also shown in Fig. 10 (open dots, preliminary values). All the new events fall in the most likely region for the QCD background.

The UA2 experiment in 1988, with a calorimetric coverage now up to $\sim 5°$ from the beams, collected 560 W events [21]. With the cuts $E_T^e \geq 20$ GeV, $E_T^{miss} \geq 20$ GeV, and $E_T^{jet} \geq 10$ GeV, and with $|\eta_{jet}| < 2.0$, they have 11 $W + \geq$2-jet events. These 11 events are also plotted in Fig. 10 (preliminary, UA2 calibrations are not final). It is legitimate to compare UA1 and upgraded UA2 data, as jet acceptances are now comparable. There is a single event (labelled D) at $M_{jet\text{-}jet} \approx 80$ GeV, which is consistent with WW production. This event also is plotted in Fig. 11, and is optimally located for the $t\bar{t}$ interpretation. A fact that is also rather intriguing is that both C and D are 3-jet events, the only ones of UA2 in 1985 and 1988 [19–21]! This might (optimistically) be taken as an indication of the expected, but difficult to observe, b-jets! However, from Fig. 10 it is clear that events D, A, and B are not a statistically significant separate population. These are—at best—hints of top production with $m_t \sim m_W$, and more data are needed. The CDF experiment has also a number of $W + \geq$2-jet events (Fig. 8c), among which it would be interesting to look for signs of open $t \rightarrow Wb$ decay; no analysis in that spirit has yet been shown.

5.4 A possible way of separating signal and background

In view of the increased statistics with the data of 1989, it is important to look for ways of differentiating between signal and background [14, 16, 17, 22]. Figure 12 shows, for example, the inclusive single-W p_T^W distribution at $\sqrt{s} = 0.63$ TeV [23], and the p_T^W spectrum in W + 2 jets for two sets of cuts and for $t\bar{t}$ production [22]. There is no significant difference in the shapes of the signal and background p_T^W spectra. However, the comparison of the shapes of the jet transverse energies

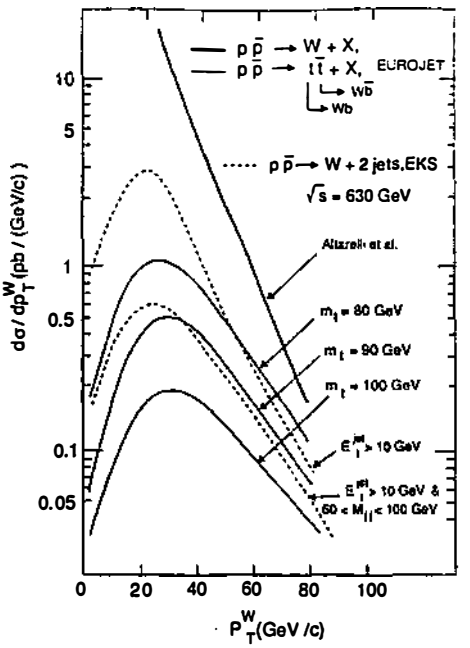

Fig. 12 Inclusive W transverse momentum $d\sigma/d_T^W$ [23], compared with $d\sigma/dp_T^W$ for $t\bar{t}$ production and for W + 2 jets, at $\sqrt{s}$ = 0.63 TeV [14, 22].

(Fig. 13) is more promising. The E_T^{jet} distribution for the two hardest jets from $t\bar{t} \to W(\to \ell\nu)$ $W(\to$ jet-jet) (the b-jets are ignored) exhibits a Jacobian peak. For W + 2 jets, it is a monotonically falling bremsstrahlung spectrum, despite the requirement that $M_{jet\text{-}jet} \approx m_W$. These two jet spectra have distinct shapes and might resolve the ambiguity [14, 16, 22]. However, for this method to be useful, it is mandatory to have reliable jet detection and measurement at low jet energies, say for $E_T^{jet} \gtrsim 10$ GeV.

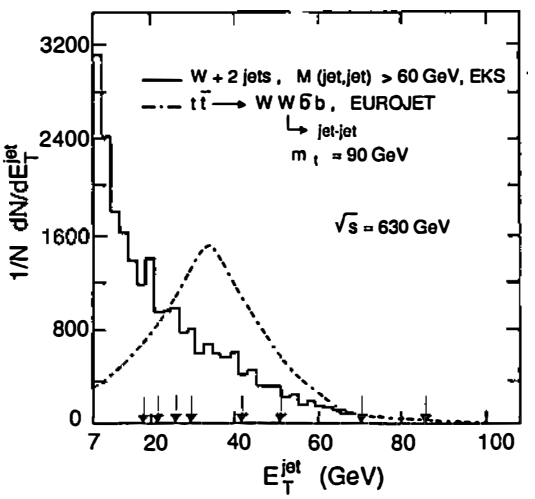

Fig. 13 Jet transverse energy distribution for W + 2 jets and for $t\bar{t} \to WWb\bar{b} \to e\nu$ + jet-jet + $b\bar{b}$ signal [14, 22]. The arrows indicate the transverse energies of the jets for the four events (A, B, C, D) of UA1/2 consistent with WW production (data up to and including 1988).

How do the jets of the four WW-consistent events compare with these spectra? They are indicated by the arrows in Fig. 13. They represent a satisfactory sampling of the expected $t\bar{t}$ distribution, but are not grossly inconsistent with the bremsstrahlung spectrum either. (The jet energy resolution should somewhat smear the bremsstrahlung spectrum.) The result is promising but statistically inconclusive, in particular as the question is not whether data can distinguish between one distribution or the other, but rather between the W + jets background (whose magnitude may be uncertain by a factor of ~ 2), with or without the additional $t\bar{t}$ contribution.

It will be most interesting to see what happens with the data of 1989, and in particular in the CDF data on lepton + ν + ≥ 2 jets. Figure 9 shows the expected rate of rise of the W + 2-jet background from $\sqrt{s}$ = 0.6 to 2.0 TeV, with three sets of cuts on jets: i) $E_T^{jet} > 10$ GeV, ii) $E_T^{jet} > 20$ GeV, and iii) $E_T^{jet} > 20$ GeV, with 60 GeV < $M_{jet\text{-}jet}$ < 100 GeV, i.e. faking a WW event [22]. The background increases with energy at least as quickly as the signal. One also sees that the apparent WW cross-section is comparable with the t-quark cross-section for $m_t \approx 90$ GeV. For $m_t \geq 100$ GeV this background will thus overwhelm the t-quark signal. In this mass range, which may be probed only at Fermilab, the observation of the b-jets should, however, provide additional rejection power. Single-W production with ≥ 3 jets should be suppressed by factors of the order of α_s per jet, whilst b-jets become hard and easily observable for $m_t > 110$ to 120 GeV [14, 17]. Thus the $80 \lesssim m_t \lesssim 110$ GeV range might be difficult in the lepton + ν + ≥ 2-jet channel, but could still be probed with the $e\mu$ channel at ~ 20 pb^{-1}. For $m_t > 100$ to 120 GeV, the ℓ + ν + ≥ 3- or 4-jet channel may take over as the most profitable one. It is clear that a good understanding of single-W production accompanied by ≥ 3 jets will be needed in order to fully exploit the mass reach of the Fermilab Collider.

6. SUMMARY AND CONCLUSIONS

Figure 14a summarizes the t-quark mass regions probed by the various experiments, with the present lower limits or mass regions excluded (solid lines). The TRISTAN limit is $m_t > 30$ GeV, and is very solid. The present $p\bar{p}$ collider limits are all at $m_t \geq 60$ GeV, making the t-quark inaccessible to the SLC or to LEP1. None of these analyses is, as yet, definitive. They all assume a standard branching ratio for $t \rightarrow e/\mu + \nu + b$ of 1/9, and depend on the now rather safe QCD calculations of $t\bar{t}$ cross-sections [4, 5] (in the case of the CERN $p\bar{p}$ Collider and $m_t \geq 50$ GeV, on $W \rightarrow t\bar{b}$ normalized to the observed $W \rightarrow \ell\nu$ mode). In Fig. 14a are also indicated (dashed or dotted lines) the mass domains we expect to be probed with the totality of data available at present or in the near future. The CERN Collider experiments are now in the $m_t \sim 50$ to 60 GeV region, and with the data of 1989 they may reach the $m_t \sim m_W$ region. The CDF experiment should approach this region with the present data in the $e\mu$ channel and, if the QCD background is well understood, could reach the $m_t \sim 100$ GeV region with the $\ell + E_T^{miss}$ + ≥ 2-jet channel. The $e\mu$ channel is probably the most suitable one for probing this difficult region.

We should also keep in mind that the ratio of $W(\rightarrow \ell\nu)$ to $Z(\rightarrow \ell\ell)$ production cross-sections, for the data up to and including 1985, favoured a t-quark in the mass range ~ 60 GeV to ≤ m_W [24]. The upper bound of $m_t \leq m_W$ suggested by this method could, however, still be evaded, due essentially to the large statistical errors on $\sigma(Z \rightarrow \ell\ell)$. If, with the new (1988/89) high-statistics data from the collider experiments, the central value of this ratio $\sigma(W \rightarrow \ell\nu)/\sigma(Z \rightarrow \ell\ell)$ turns out to be ≤ 8 (see discussion in Refs. [8] and [24])—which should soon be clarified—a limit at $m_t \leq m_W$ would be difficult to avoid! This would suggest that the t-quark is just above the lower bound discussed here, and in the mass range now being explored by UA1, UA2, and CDF with the data of

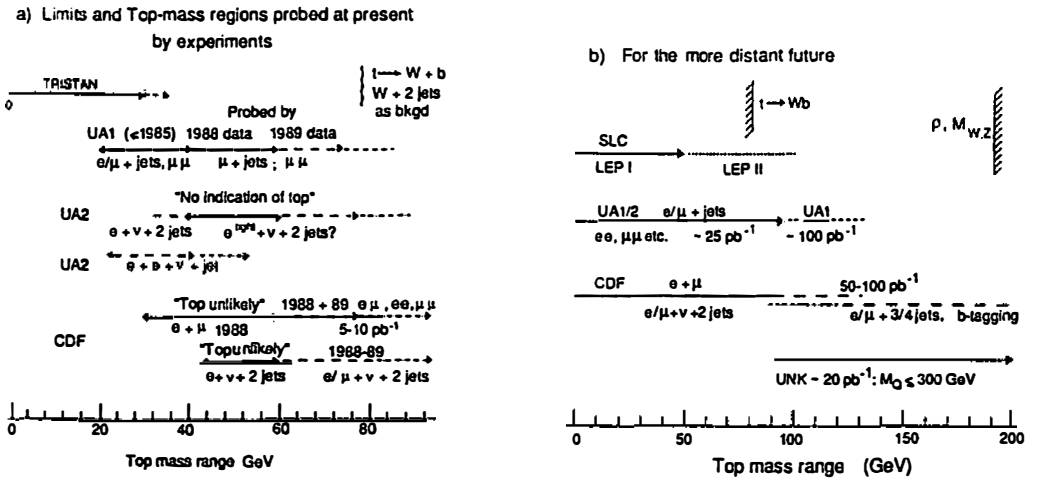

Fig. 14 a) Top-quark mass regions excluded or probed by present experiments in the various decay channels, and expectations for the near future; b) in the foreseeable future, with the experimental sensitivities indicated.

1989, thus promising a very lively summer! This possibility (with m_t in the ~ 70 to 80 GeV range) may not be in contradiction with the few peculiar events of UA1 and UA2 discussed previously. For $m_t \gtrsim 70$ GeV, $t\bar{t}$ is already more efficiently detected than $t\bar{b}$ [7], and the kinematics of these events is not sufficiently constrained to exclude quasi-WW events slightly below threshold [14, 16, 17], since only the transverse mass is measured for the lepton–neutrino system, and the jet–jet effective mass resolution is ~ 15%. The measurement of this ratio should be eagerly awaited and may have most interesting implications.

Keeping all options open, we indicate in Fig. 14b the mass regions that will be explored by the SLC and LEP, and the expectations for UA1 and UA2 with luminosities of ~ 25 pb^{-1}, and for CDF or D0 with comparable experimental sensitivities. The e^+e^- experiments, although more limited in the potential mass range, are important, as the current $p\bar{p}$ collider limits would collapse if it turned out that the assumed t-quark semileptonic branching ratios were badly overestimated. This might be the case if there exists a light charged scalar boson with mass $< m_t$ [25]. Barring this last possibility, if $m_t > 100$ to 120 GeV, only Fermilab has a chance of exploring this mass region, and luminosities of the order of 50 to 100 pb^{-1} will be needed to cover it up to the current upper bound, $m_t \lesssim$ 200 GeV [26]. This will probably be done in the $\ell + E_T^{miss} +$ ≥ 3- or 4-jet channel, and b-jet recognition and tagging may be required to suppress the W + multijet QCD background. On this time scale (up to ~ 1995), a 6 TeV machine such as UNK (Serpukhov) with a sensitivity of ~ 20 pb^{-1} could reach a t-quark (or higher-generation heavy quark) mass region of ~ 300 GeV.

* * *

REFERENCES

[1] S. Igarashi et al. (AMY Collab.), Phys. Rev. Lett. **60** (1988) 2359.
I. Idashi et al. (TOPAZ Collab.), Phys. Rev. Lett. **60** (1988) 97.
H. Yoshida et al. (VENUS Collab.), Phys. Lett. **B198** (1987) 570.

[2] T. Tsuboyama (VENUS Collab.), to appear in Proc. 24th Rencontres de Moriond, 1989.
L. Piilonen, presented at the 12th Int. Workshop on Weak Interactions and Neutrinos, Ginosar, Israel, April 1989.

[3] C. Albajar et al. (UA1 Collab.), Z. Phys. **C37** (1988) 505.

[4] G. Altarelli, M. Diemoz, G. Martinelli and P. Nason, Nucl. Phys. **B308** (1988) 724.

[5] P. Nason, S. Dawson and K. Ellis, Nucl. Phys. **B303** (1988) 607.

[6] C. Albajar et al. (UA1 Collab.), Status of the UA1 top-quark search, CERN-EP preprint in preparation, June 1989.
J.P. Revol, *in* Proc. Rencontres de la Vallée d'Aoste, La Thuile, 1989.
M. Della Negra, to appear in Proc. 24th Rencontres de Moriond, 1989.
G. Sajot, Search for the Top-Quark with UA1, to appear in Proc. 12th Int. Workshop on Weak Interactions and Neutrinos, Ginosar, Israel, April 1989.

[7] J.P. Repellin, to appear in Proc. Rencontres de la Vallée d'Aoste, La Thuile, 1989.
S. Grunendahl, Top search in UA2, to appear in Proc. 24th Rencontres de Moriond, 1989.
P. Wells, Top search in UA2, ibid.
M. Moniez, Recent results from UA2, to appear in Proc. 12th Int. Workshop on Weak Interactions and Neutrinos, Ginosar, Israel, April 1989.

[8] A. Barbaro-Galtieri, The search for the top quark, to appear in Proc. 8th Int. Conf. on Physics in Collision, Capri, 1988.

[9] D. Baden, Search for top at CDF, to appear in Proc. 24th Rencontres de Moriond, 1989.
M. Shochet, Search for the top quark in CDF, to appear in Proc. Rencontres de la Vallée d'Aoste, La Thuile, 1989.
R.G. Wagner, to appear in Proc. 12th Int. Workshop on Weak Interactions and Neutrinos, Ginosar, Israel, April 1989.

[10] C. Albajar et al. (UA1 Collab.), Z. Phys. **C37** (1988) 489.
C. Albajar et al. (UA1 Collab.), Phys. Lett. **B213** (1988) 405.

[11] S.D. Ellis et al., Phys. Lett. **B154** (1985) 389.

[12] P. Colas and D. Denegri, Phys. Lett. **B195** (1987) 295.

[13] C. Albajar et al. (UA1 Collab.), Phys. Lett. **B193** (1987) 389.

[14] D. Denegri, Hadroproduction of top for $m_t \sim m_W$, preprint CERN-EP/89-39 (1989), to be published in Proc. Workshop on Heavy Flavour Physics, Erice, 1988.

[15] H. Fritzch, Phys. Lett. **B166** (1986) 423.
J. Ellis and G. Fogli, Phys. Lett. **B213** (1988) 526.
C.H. Albright, Top quark mass bounds in the hierarchical chiral symmetry-breaking framework, LAPP (Annecy) report LAPP-TH-251/89 (1989), and references therein.
D. Haidt, Status of the electroweak standard model, to appear in Proc. 12th Int. Workshop on Weak Interactions and Neutrinos, Ginosar, Israel, April 1989.

[16] S. Gupta and D.P. Roy, Z. Phys. **C39** (1988) 417.
R. Kleiss et al., Z. Phys. **C39** (1988) 393.
H. Baer, V. Barger, H. Goldberg and R.J.N. Phillips, Top quark signatures at the Tevatron Collider, Univ. Wisconsin report, MAD/PH/367 (1987), and references therein.
F. Halzen et al., Top quark signatures at the Tevatron Collider, Univ. Wisconsin report MAD/PH/436 (1988).
I. Bigi et al., Production and decay properties of ultraheavy quarks, SLAC-PUB-4021 (1986).
H. Baer, V. Barger and R.J.N. Phillips, Top quark detection via W + n jet measurements, Univ. Wisconsin report MAD/PH/458 (1988) and Florida State Univ. report FSU-HEP-88 1208 (1988).

[17] R. Kleiss et al., Z. Phys. **C39** (1988) 393.
V. Barger et al., Large p_T weak boson production at the Tevatron, Univ. Wisconsin report MAD/PH/455 (1988).
J.L. Rosner, Enrico Fermi Inst. report EFI-89-02 (1989).

[18] A. Ali et al., Nucl. Phys. **B292** (1987) 1.

[19] P. Bagnaia et al. (UA2 Collab.), Phys. Lett. **B139** (1984) 105.

[20] R. Ansari et al. (UA2 Collab.), Phys. Lett. **B194** (1987) 158.

[21] M. Bonesini (UA2 Collab.), W and jets in the UA2' 1988 run, to appear in Proc. 24th Rencontres de Moriond, 1989.

[22] B. Andrieu and D. Denegri, UA1 internal report: Meeting of the Working Group on UA1 at high luminosity, 1988.
B. Andrieu, Ph.D. thesis, Collège de France, 1989.

[23] G. Altarelli et al., Z. Phys. **C27** (1985) 617.

[24] C. Albajar et al. (UA1 Collab.), Phys. Lett. **B198** (1987) 287, and references therein.
R. Ansari et al. (UA2 Collab.), Phys. Lett. **B198** (1987) 440.
F. Halzen, Phys. Lett. **B182** (1986) 388.
P. Colas et al., Z. Phys. **C40** (1988) 527, and references therein.
D. Denegri, B. Sadoulet and M. Spiro. The number of neutrino species, preprint CERN-EP/89-72 (1989).
V. Barger, to appear in Proc. 12th Int. Workshop on Weak Interactions and Neutrinos, Ginosar, Israel, April 1989, and references therein.

[25] S.L. Glashow and E. Jenkins, Phys. Lett. **B196** (1987) 233.
V. Barger and R.J.N. Phillips, Phys. Lett. **B201** (1988) 553.

[26] U. Amaldi et al., Phys. Rev. **D36** (1987) 1385.
G. Costa et al., Nucl. Phys. **B297** (1987) 244.
K. Einsweiler and S. Weidberg, Standard model parameters from UA1 and UA2, preprint CERN-EP/88-152 (1988).